EFDA–JET–PR(07)43

P. Belo, W. Fundamenski, V. Parail, G Corrigan, C. Giroud, J. Spence
and JET EFDA contributors

Numerical Simulation of Hydrogenic and Impurity Flows in the Boundary Plasma on JET

Numerical Simulation of Hydrogenic and Impurity Flows in the Boundary Plasma on JET

P. Belo[1], W. Fundamenski[2], V. Parail[2], G Corrigan[2], C. Giroud[2], J. Spence[2]
and JET EFDA contributors*

JET-EFDA, Culham Science Centre, OX14 3DB, Abingdon, UK

[1]EURATOM/IST Fusion Association, Centro de Fus„o Nuclear, Av. Rovisco Pais 1049-001 Lisbon Portugal
[2]EURATOM-UKAEA Fusion Association, Culham Science Centre, OX14 3DB, Abingdon, OXON, UK
** See annex of M.L. Watkins et al, "Overview of JET Results ",*
(Proc. 21 st IAEA Fusion Energy Conference, Chengdu, China (2006)).

Preprint of Paper to be submitted for publication in
Plasma Physics and Controlled Fusion

ABSTRACT

Impurity seeding of recycling impurities such as Neon or Argon, or non-recycling impurities such as Nitrogen, is an essential element of power exhaust in future fusion reactors, including ITER. Aside from increasing the fraction of power radiated onto the main chamber, thus reducing the fraction carried by the plasma to the divertor, it also provides a viable method of ELM size reduction (mitigation) in ELMy H-mode plasmas. However, impurity seeding raises the risk of impurity accumulation in the core of the plasma, which degrades reactor performance and can lead to thermal collapse of the discharge. It is therefore imperative to understand the mechanisms of impurity transport in the boundary plasma, including the close field line (edge) region and the open field line (Scrape-off Layer or SOL) regions, and specifically, to quantify impurity influx across the magnetic separatrix and the 'screening' effect of the SOL. In this paper, we employ the two-dimensional transport code EDGE2D/NIMBUS to investigate the influence of (anomalous) parallel SOL flows, observed experimentally on JET and other tokamaks, on the 'screening' of a recycling impurities (Neon). The parallel SOL flow is adjusted by external momentum injection, such that Mach number at the top of the vessel $M_{||}^{top}$ varies from ~0 to ~0.5. Simulations indicate that the deuterium density in the plasma core increases by ~50 % over this range, in agreement with experimental finds (comparing normal and reversed field discharges). Notably, this density increase is associated with (caused by) plasma compression on the inboard side of the torus caused by the parallel SOL flow, thus leading to inverted radial density gradient and a recirculating flow patter (convective cell) linking the inboard and outboard SOL regions. Simulations predict a 5 % decrease of impurity (Neon) concentration in the plasma core when the deuterium flow at the top of the vessel increases to Mach number, $M_{||}^{top} \sim 0.2$, with little change for higher Mach numbers.

1. INTRODUCTION

Impurity accumulation in the plasma core, which can lead to a reduction of the fusion power and to the possibility of radiative collapse of the plasma discharge, is one of the main concerns in the design of plasma scenarios for future fusion reactors. Plasma impurities are typically divided into two categories: intrinsic and extrinsic. *Intrinsic* impurities include the ash of the burning plasma (alpha particles or Helium ions when thermalised) and material eroded from the vessel walls and divertor tiles due to plasma-wall interaction. *Extrinsic* impurities are those purposely added to the plasma, e.g. to increase the radiative power fraction and reduce the size of Edge Localised Modes (ELMs); the latter effect, known as *ELM mitigation*, is important to avoid extreme transient thermal loads during the ELM that can lead to excessive damage of first wall components [2]. For instance, Argon, Neon and Nitrogen were introduced as extrinsic impurities on JET in the attempt to mitigate ELMs by increasing of impurity radiation from the boundary plasma [3, 4]. In these discharges, especially those with high triangularity, impurity concentration in the plasma core was found to increase when the level of the deuterium gas puff decreased below a certain critical level, see Fig.1 (it is worth remembering that strong deuterium gas puffing (fuelling) has detrimental effects on plasma

performance, since it reduces the pedestal temperature, i.e. cools the edge plasma, and therefore degrades plasma confinement, e.g. from type-I to type-III ELMy H-mode [5, 6]). This increase in impurity concentration was explained in ref. [1] by the dominant role of the neoclassical flow within the Edge Transport Barrier (ETB), which reverses sign of the neo-classical impurity convective velocity from outward- to inward-directed (from outflow to inflow) when the absolute value of the normalized radial gradient of the deuterium ion density, $\left|\frac{1}{n_i}\frac{dn_i}{dr}\right|$, increased above some critical value, proportional to the normalized radial gradient of the ion temperature, $\left|\frac{1}{T_i}\frac{dT_i}{dr}\right|$ (the ratio of the two gradients clearly varied with the level of deuterium gas puffing). However, such neo-classical *outflow* within the ETB does not entirely shield the plasma from impurity *inflows*, which can still diffuse into the plasma core provided the impurity density at the separatrix is sufficiently high. Therefore, to prevent plasma contamination by extrinsic (and to a less extent, by intrinsic) impurities, it is necessary to ensure that these impurities are effectively 'screened' by the Scrape-Off Layer (SOL), such that their density at the separatrix is sufficiently low.

There are two parallel transport processes in the SOL that can control the degree of *impurity screening*: (i) impurities experience a *frictional force* towards the target plates by collisional drag with the flow of deuterium ions. This flow tends to compress the impurities at the target plates, allowing them to be pumped away more efficiently; (ii) collisional friction is counteracted by the parallel component of the *thermal force*, which usually drives impurities in the opposite direction, away from the target plates. The overall impurity behaviour is controlled by the balance between these two forces. It is therefore important to investigate the flow pattern of hydrogenic (deuterium) ions in the boundary plasma, and particularly in the SOL.

As has been observed on many tokamaks, the hydrogenic plasma flow in the SOL is strongly sensitive to the toroidal magnetic field direction, or alternatively, to the direction of the vector $\mathbf{B}\times\nabla$B, i.e. of the 'grad-B' drift of ion guiding centres. Here the following conventions is typically used: when $\mathbf{B}\times\nabla$B points towards the X-point (divertor) the toroidal magnetic field is said to be in the *normal*, or *forward*, direction, and when it points away from the X-point, it is said to be in *reversed* direction. Measurements on JET, which is equipped with a reciprocating Mach probe near the top of the vessel, and thus able to measure SOL flows at that poloidal location (this flow is typically expressed in terms of the parallel Mach number at the top of the vessel, $M_{||}^{top} = v_{||} / c_s$, with c_s being the plasma sound speed, $v_{||}$ is the parallel thermal velocity), indicate a strong flow ($M_{||}^{top} \sim 0.5$) towards the *inner* divertor in discharges with *normal* toroidal field direction, and a weak flow ($M_{||}^{top} \sim -0.1$) towards the *outer* divertor in discharges with *reversed* toroidal field direction [7]. These observations are consistent with those made on other machines [8], equipped with SOL Mach probes at other poloidal locations, e.g. the outer mid-plane, the inner mid-plane or outer and inner divertor regions [8]. The resulting picture suggests that the stagnation point of the deuterium parallel SOL flow moves from some region between the outer mid-plane and the outer X-point (with normal field direction) to vicinity of the machine top (with reversed field direction) [8].

While a satisfactory explanation of this difference in the parallel flow pattern is yet to emerge, there is a wide consensus that Guiding Centre (GC) drifts must play an important role in the answer. Unfortunately, up to date EDGE2D/NIMBUS simulations including the effect of GC-drifts [9] were only able to qualitatively reproduce the radial profiles of $M_{||}^{top}$, not its magnitude (indeed, this magnitude of this flow, which becomes trans-sonic or even super-sonic at the inner mid-plane, has prompted the label *anomalous* to be associated with this parallel SOL flow). Indeed, the examination of the total number of neutrals being ionised inside the separatrix has revealed that this magnitude can only be matched in the presence of a significant re-cicrulating flow (convective cell) linking the inboard and outboard SOL regions [10]. Recently it was suggested that such a re-circulating flow pattern could be partly caused by the ballooning nature of the edge-SOL turbulence, in which the over-pressurisation of local SOL flux tubes naturally drives a plasma flow towards the inner divertor [11]; this hypothesis was then reinforced by Edge-SOL ELectrostatic (ESEL) turbulence simulations for TCV and JET [11].

It is noteworthy that despite the pronounced difference in the parallel SOL flow pattern between normal and reversed field directions, little (if any) difference in the Carbon impurity screening was observed [12] (here the experiments were performed under L-mode conditions). Since Carbon is an intrinsic impurity, it is difficult to establish if the Carbon content inside the separatrix is a result of changes to the *transport* processes in the edge/SOL or due to changes in sources of Carbon, e.g. physical and chemical sputtering in the divertor and wall regions [8]. This uncertainty in the interpretation of the intrinsic impurity (Carbon) results, makes it difficult to extrapolate these results to the case of extrinsic impurities (Neon, Argon or Nitrogen). One may expect that the interpretation of extrinsic impurity screening would be simplified by the fact that the source (inflow) of the impurity into the plasma can now be (at least partly) controlled. Unfortunately, there is at present no data, i.e. no experiments, with Neon or Argon injection with reversed magnetic field. We are therefore confined to simulating the effect of anomalous parallel SOL flow on the screening of *extrinsic* impurity and then comparing the numerical results with *intrinsic* impurity (Carbon) experiments, in order to draw some conclusions as to the relative contributions of SOL transport and surfaces sources (sputtering, ablation, etc.).

Consequently, the rest of the paper is dedicated to a numerical study of extrinsic impurity (Neon) screening by anomalous parallel SOL flow, using the two-dimensional plasma fluid transport code EDGE2D/NIMBUS [9]. This code solves the plasma fluid equations in a realistic magnetic geometry, including both edge and SOL regions, see Fig.2; note that the two directions include the poloidal direction, representing the combination of diamagnetic and parallel transport along the flux surface, and the radial direction, representing transport perpendicular to the flux surface. While parallel (and poloidal) transport coefficients are based on the (Spitzer-Härm)-Braginskii expressions, radial transport coefficients are prescribed arbitrarily, since the governing turbulent processes cannot at present be properly quantified [13]. The fluid EDGE2D is coupled to a Monte-Carlo code, NIMBUS, which follows neutral particle trajectories and thus calculates the particle and energy sources and

sinks due to neutrals recycled at divertor targets and chamber walls. The computational domain of EDGE2D/NIMBUS comprises the entire SOL, the private region below the X-point and a small region inside the separatrix that incorporates the Edge Transport Barrier (ETB) region in H-mode. The computational grid, or mesh, is produced based on an EFIT reconstruction of the magnetic equilibrium using the grid generator code GRID2D. The grid used in the simulations is plotted in Figure 2.

Guided by ref [12], we include an ad hoc model for anomalous parallel SOL flow in the EDGE2D/NIMBUS code, by imposing an additional external source of parallel momentum into the SOL region. Directing the momentum source towards the inner target and varying its magnitude, it is possible to reproduce the anomalous parallel SOL Mach number measured under typical L-mode conditions.

This method was not used to simulate H-mode plasmas, since the Mach probes, which are the main tool to measure the flow velocity, become emissive in these high power density plasmas decreasing the signal to noise level. However, it is possible to infer the existence of strong parallel SOL flow in the H-mode plasmas with reversed magnetic field [11]. Since the anomalous parallel SOL flow and its profile are not known for H-mode plasmas, we will scan the amplitude of $M_{||}^{top}$ to study its influence on extrinsic impurity screening.

The paper is organised as follows: Section 2 describes the model used in the simulations, Section 3 presents the results for deuterium and Neon, and Section IV draws the conclusions.

2. PREDICTIVE MODELLING

The above code package was used to model the boundary plasma of a deuterium fuelled discharge for typical JET H-mode plasma with the MARKIIGB divertor [11].

As already mentioned, the radial transport in EDGE2D/NIMBUS is prescribed in an ad-hoc fashion, with the Braginskii's expressions only used for parallel flows. The ad-hoc radial transport is prescribed at values typical for H mode plasmas, with equal coefficients for all ion species; in particular, equal radial heat diffusivities are assumed for ions and electrons, $\chi_{\perp i} = \chi_{\perp e}$. The particle and heat diffusivities are specified with a radial profile, with different values in the plasma core, the ETB and SOL regions. In the plasma core (up to the top of the ETB), the particle diffusivity was chosen as $D_\perp = 0.5\ m^2/s$ and thermal diffusivities as $\chi_{\perp i,e} = 1.5\ m^2/s$ (values obtained from JETTO simulations using the Bohm/GyroBohm empirical transport model for the same JET pulse [1]). Within the ETB, these values are decreased by an order of magnitude to $D_\perp = 0.05\ m^2/s$ and $\chi_{\perp i,e} = 0.05\ m^2/s$ (close to the neo-classical ion heat diffusivity), and in and in the SOL they are increased again to $D_\perp = 0.25\ m^2/s$ and $\chi_{\perp i,e} = 0.35\ m^2/s$ (these values are in the range normally used in EDGE2D/NIMBUS modelling [14], and are typically needed to obtain agreement with divertor target plasma profiles). To focus on the influence of the SOL on impurity screening, the radial neoclassical flow for impurities was assumed to be vanishingly small within the ETB in all these simulations.

The anomalous parallel SOL flow was introduced into EDGE2D/NIMBUS by adding an external source of parallel momentum directed towards the inner divertor target. In order to reproduce the

experimental observations [15], this force was applied in the poloidal direction over the relatively small poloidal segment from the outer mid-plane to the vessel top [8], i.e. between 12 o'clock and 3 o'clock of the poloidal cross-section. The radial profile of this force, as shown in figure 3a, indicates a zero force inside the separatrix, rising to a peak value of 5 mm beyond the separatrix and vanishing again 11mm from the vessel wall. This force could in principle be made to act on both deuterium ions and impurities. For the sake of simplicity, we only considered the force acting on deuterium ions; earlier EDGE2D/NIMBUS simulations showed that the result did not change significantly when this force was also applied to the impurities [12]. The peak value of the force magnitude acting on ions was varied from zero to a maximum value of 170 Nm^{-3}, figure 3a, which corresponds to a maximum parallel Mach number of $M_{||}^{top} \sim 0.5$ at the top of machine vessel, see Fig.3b. This figure also shows the radial profiles of $M_{||}^{top}$ caused by the applied forces with different amplitudes.

In all simulations, the deuterium ion density, n_i, was feedback-controlled by gas puffing such that its separatrix value, i.e. its value at $r = a$, satisfied $n_i(a) \approx 3.5\times10^{19}$ m^{-3}. The deuterium was injected at the high field side (inner mid-plane puff) or at the low field side (outer mid-plane puff), see Fig.2. The level of required gas puffing was influenced by both the specified deuterium density at the outer mid-plane and the imposed external momentum source.

Neon was injected locally from the outboard side, beneath the inlet for the deuterium puff, see Figure 2, as was the case in the relevant JET experiments. The total content of Neon was held fixed at 3.1×10^{18} particles in the whole computational volume of $25m^3$. This level of Neon corresponds to less than 1% of the total ion content and increases Z_{eff} to a maximum level of $Z_{eff} \leq 1.3$.

3. RESULTS

The EDGE2D/NIMBUS simulations show a large difference in deuterium parallel SOL flow pattern in the cases without, figure 4a, and with, figure 4b, the external momentum source. The two figures indicate an influence of the momentum source on the stagnation point of this flow and on the asymmetry of the flows entering the inner and outer divertor volumes. The inclusion of the momentum source moves the stagnation point closer to the X-point (Fig.4b), consistent with observations [8].

The question then arises, as to the influence of this external momentum on the deuterium ion density n_i and electron and ion temperatures, T_e and T_i, in the ETB and divertor regions, and on the screening of impurity ions from the plasma core. Recall that changes of (n_i, T_e, T_i)-gradients within the ETB can alter the direction of the neoclassical velocity of impurities and hence their concentration inside the separatrix [1]. Similarly, the change in the electron temperature in the divertor region can change the degree of divertor plasma detachment. These issues were explored using the simulations, with the obtained results presented below.

3.1 DEUTERIUM ION DENSITY, N_i

The deuterium ion density profiles at the outer and inner mid-planes for a series of simulations with different amplitudes of external source of momentum applied in the SOL are plotted in figure 5.

This figure clearly indicates that n_i inside separatrix, and specifically at the top of the ETB (pedestal), increases with $M_{||}^{top}$. It also shows that n_i at the *outer* mid-plane (low field side), n_i^{omp}, decreases with radius for all values of $M_{||}^{top}$, and that (the negative of) its radial gradient, $-dn_i^{omp}/dr > 0$, increases with $M_{||}^{top}$ in the ETB region and remains roughly constant in the SOL, see figure 5b. In contrast, n_i at the *inner* mid-plane (high field side), n_i^{imp}, decreases with radius for $M_{||}^{top} < 0.2$, while for $M_{||}^{top} > 0.2$, it increases with radius, i.e., its radial gradient, dn_i^{imp}/dr, becomes positive in the ETB region, and is again unaffected in the SOL, see Fig.5a. As a result, n_i^{omp} at the separatrix remains constant, while at n_i^{imp} at the separatrix increases with $M_{||}^{top}$.

In all the above simulations the deuterium gas was injected from the outer mid plane. However, the results of n_i and $M_{||}^{top}$ profiles did not change noticeably when the deuterium gas was injected from the inner mid plane. The only significant difference occurred in the far SOL, where the deuterium density decreased at the low field side, and increased at the high field side, when the inlet location was moved from the outer to the inner mid plane.

This increase of n_i at the top of the ETB (pedestal) with $M_{||}^{top}$ was also observed experimentally on JET based on a comparison of two similar H-mode discharges, one with normal (58570) and the other with reversed (Pulse No: 59636) magnetic field direction, the former exhibiting $M_{||}^{top} \sim 0.5$, the latter $M_{||}^{top} \sim -0.1$, see figure 6. This figure shows the time traces of two line integrated electron densities at central and edge lines of sight, $r/a|_{\min} = 0.05$ (figure 6a) and $r/a|_{\min} = 0.08$ (figure 6b). Both the edge and core densities are higher in the normal field discharge, which can be interpreted as an increase of density with parallel Mach number, as predicted in figure 5. Also shown in figure 6 are the time traces of deuterium gas fuelling rates (figure 8c). It is noteworthy that the pulse with *higher* level of fuelling (59636, reversed field), exhibits a *lower* electron density, in contrast to the normally observed trend of plasma density increasing with fuelling rate. Hence, the decrease in the edge density in Pulse No: 59636, as compared to Pulse No: 58570, cannot be attributed to a difference in the fuelling rate, but must be related to a difference in the boundary plasma flow pattern, in particular to presence of a strong parallel SOL flow at the top of the vessel.

Returning to the analysis of EDGE2D/NIMBUS simulations, we observe (see figure 7) that the radial deuterium ion flow, which is normally positive (an outflow) on both inboard and outboard sides, becomes negative (an inflow) on the inboard side when even a small amount of external parallel momentum is injected into the SOL, e.g. this effect is observed even for a modest parallel Mach number, $M_{||}^{top} \sim 0.15$. Figure 7 also indicates that without external momentum injection, deuterium ion inflow across the separatrix only occurs in the vicinity of the X-point. The surface area of a net inflow region is thus greatly extended when $M_{||}^{top} > 0.1$, thus explaining the increase of n_i inside the separatrix.

This radial flow reversal across the separatrix on the inboard side of the torus, suggests that the external force creates a re-circulating flow (convective cell) involving the inboard and outboard regions, coupled via the SOL and ETB regions. Such a convective flow pattern is indeed observed in the simulations with external momentum injection, see figure 8b combined with figure 4b. Without external

source of momentum the radial flow across the separatrix is directed outward everywhere except in the X-point region, figure 8a. Note that the radial flow pattern shown in figure 8 is consistent with the poloidal profiles shown in figure 7.

As expected, the deuterium flow to the inner target increases, and that to the outer target decreases, with $M_{||}^{top}$ representing SOL flow towards the inner target, see figure 9. This change in the imbalance (in-out asymmetry) between the flows to the inner and outer targets was likewise observed experimentally on JET, in the two discharges discussed above, see figure 10, although in this case the imbalance was mainly associated with a strong decrease of the flow to the outer target in the discharge with the normal magnetic field (Pulse No: 58570).

3.2. ELECTRON TEMPERATURE

As already mentioned, EDGE2D/NIMBUS simulations indicate that the deuterium density at the inner (outer) target and the plasma flow to that target increase (decrease) with $M_{||}^{top}$. On the other hand, the plasma pressure at the inner target does not change significantly with $M_{||}^{top}$, while at the outer target it decreases with $M_{||}^{top}$. This means that the electron temperature at the inner target must decrease with $M_{||}^{top}$, as indeed it does, see figure 11. In contrast, the electron temperature at the outer target decreases with $M_{||}^{top}$, accompanied by a reduction in the electron pressure (by a factor of 5) and of the associated parallel electron energy flow, Q_e,

$$Q_e = \underbrace{\frac{5}{2}\, n_e\, T_e\, v_{||}}_{Conective} - \underbrace{n_e\, \chi_{||e}\, \nabla T_{||}}_{Conductive}$$

where $\chi_{||e}$ is the parallel electron heat diffusivity and $v_{||}$ is the parallel thermal velocity. In EDGE2D/NIMBUS a positive Q_e indicates energy flowing into the target, i.e. a heat load on the target.

Convective and conductive contributions to the energy flows towards the inner and outer divertors are shown in figure 12a and figure 12b, respectively. The former indicates that the convective energy flow changes sign from positive (towards the target) to negative (away from the target) in the outer SOL when the external force is applied. This is because the direction of the deuterium ion flow changes from directed towards the outer divertor target to one directed towards inner target. This flow reversal, associated with the change of sign of the convective energy flow contribution, leads to a decrease of the total energy flow to the outer divertor SOL, and consequently the electron temperature decreases at the outer target, as seen in figure 11.

This reduction in the plasma temperature has an important consequence for the onset of divertor plasma detachment, which in EDGE2D/NIMBUS simulations, typically occurs when the target electron temperature drops below ~ 1 eV [16, 17]. The fact that the anomalous parallel SOL flow increases the density, and decreases the temperature, at the inner target, indicates that as $M_{||}^{top}$ increases, plasma detachment occurs at lower deuterium separatrix density, i.e. that it is easier to detach the inner divertor plasma; based on the observations above, the same is also true for the outer divertor plasma.

3.3. IMPURITIES

To study the effect of the anomalous parallel SOL flow on extrinsic impurities, Neon atoms were injected into the EDGE2D/NIMBUS simulations at the outer mid-plane, with different levels of external momentum input and deuterium fuelling first at the Outer Mid-Plane (OMP) and then, in separate simulations, at the Inner Mid-Plane (IMP).

The resulting radial profiles of the sum of the densities of all ionization states of Neon, $n_{Ne} = \sum_j n_{Ne}^{j+}$, at the inner and outer mid-plane for different values of $M_{||}^{top}$ are shown in figure 13 (for outboard injection) and figure 14 (for inboard injection).

Figure 13 (outboard Neon injection) shows that n_{Ne} is slightly higher inside the ETB for the case without external momentum injection than for the cases with finite momentum injection, i.e. for $M_{||}^{top} = 0$ compared to $M_{||}^{top} > 0.15$. It also shows that the radial gradient of n_{Ne} (at both the IMP and OMP) is only moderately affected by the anomalous deuterium SOL flow. In particular, the core and SOL profiles are quite similar, with only the ETB region noticeably affected. Note that dn_{Ne}/dr becomes positive for $M_{||}^{top} > 0.15$ in (some part of) the ETB region at both the IMP and OMP; for $M_{||}^{top} = 0$, this positive gradient is only observed at the IMP, with a decaying n_{Ne} at the OMP. The explanation to this comes from the observation that Neon particles are transported from the outboard SOL to inboard SOL by the imposed anomalous flow. Note that there is no external source of momentum on the inboard side, where only the parallel frictional and thermal gradient forces remain. Since the latter is typically larger, Neon accumulates in the inboard SOL rather than being dragged to the inner target, which explains why $dn_{Ne}/dr > 0$ in this region.

Figure 14 (inboard Neon injection) shows a strong effect of external momentum injection on the radial Neon profiles, most of this change arising for a very moderate change of $M_{||}^{top}$, from 0 to 0.15. For $M_{||}^{top} = 0$, n_{Ne} is highest in the SOL at the OMP, decreasing both radially across the separatrix and poloidally towards the IMP. Since n_{Ne} inside the ETB is roughly constant along flux surfaces, the radial profile at the IMP decreases ($dn_{Ne}/dr < 0$) in the ETB region, while that at the IMP increases ($dn_{Ne}/dr > 0$) across the ETB. For $M_{||}^{top} > 0.15$, n_{Ne} in the SOL at the OMP decreases, while that at the IMP increases, compared to the $M_{||}^{top} = 0$ case. In contrast, the core densities are only moderately affected by changing $M_{||}^{top}$, and the radial profiles across the ETB are modified to provide continuity between the core and SOL profiles. As a result, dn_{Ne}/dr changes sign across the separatrix (and inside the ETB) at both the IMP and OMP, increasing with radius at IMP ($dn_{Ne}/dr > 0$) and increasing with radius at OMP ($dn_{Ne}/dr > 0$).

To understand the above behaviour, specifically the role of outboard vs. inboard Neon injection, we should note that the $M_{||}^{top} = 0$ simulation remains unchanged if one replaces the friction force from external momentum by the friction force created by the deuterium gas puff. The only difference between the two cases, comes from the sign of the friction force in the case of the gas puffing depends on the position of the gas inlet. If the gas puff increases the friction force by changing the position of the deuterium puff from the outer to the inner mid-plane should create a positive gradient at the outer mid-plane.

Comparing impurity density profiles for the simulations with the different amplitudes of anomalous velocity, figures 13 and 14, on can see that they are very similar for the whole range of external source of momentum amplitudes. This leads us to the conclusion that in the presence of anomalous parallel SOL flow impurity density profile is practically independent on the deuterium puff position, as was indeed reported for JET plasmas [18]. This is because even for a small level of the anomalous parallel SOL momentum (above M = 0.17 at the outer mid-plane) has one order of magnitude higher flow than the classical flow velocity (which is around M = 0.02).

As it is mentioned earlier, the total Neon density inside the ETB decreases, although not significantly and its concentration decreases, see figure 15, when the external force is applied in the simulations and this increase is independent on the deuterium gas puff position, see figures 13 and 14. The possible explanation to this result is the existence of convective cells, which are observed on the patterns of the average impurity velocity in all the cases (see figure 16a for the case without the external source of momentum and figure 16b with the anomalous parallel SOL flow). The latter case has just one convective cell similar to what is observed in the deuterium flux; see the perpendicular component of the impurity flow in figure 17b (case with anomalous parallel SOL flow). On the other hand for the case without anomalous parallel SOL flow at least three convective cells are observed. This is also re-enforcing in the flow pattern using only the perpendicular component of the impurity flow, figure 17a (case without anomalous parallel SOL flow). Since impurities are forced to enter the plasma core between these cells, impurity content in the plasma core increases with the number of cells.

We observed from the EDGE2D/NIMBUS simulations that there is practically no change in impurity content inside separatrix with different values of the flow velocity. This can suggest an explanation to why no significant change of the impurity screening between JET L-mode plasmas with reversed filed and normal field was observed experimentally [9]. It is not possible to draw similar conclusion for H-mode plasmas because impurity screening in the H mode plasma depends also on n_i and T_i gradients within the ETB. Changing the balance between these two gradients can lead to a change of the impurity neoclassical convective velocity sign [1]. Full study with both effects in the SOL and ETB can only be done by using an integrated code for the edge and core transport, COCONUT. The results of this study will be published else where.

SUMMARY AND CONCLUSIONS

The influence of the SOL flows on impurity screening was studied numerically. A 2D SOL transport code EDGE2D/NIMBUS was used for the analysis of multispecies JET H-mode plasma with a typical MARKIIGB divertor configuration. An *adhoc* transport model for heat and particle perpendicular transport coefficients was used in simulations, which has been previously tested on wide range of JET plasmas. The Braginskii's equations were used for parallel transport. The anomalous parallel flow was included as external source of momentum in a way similar to what was done in ref [12].

Experimentally a much higher deuterium flux to the inner divertor target than to the outer divertor

target was observed in almost all the JET pulses [7]. This was also observed in the EDGE2D simulations with the anomalous parallel SOL flow. The other point is that for these simulations the stagnation position of the deuterium flux is in the same region between the outer strike point and the outer mid-plane that was observed experimentally in several machines [8].

The JET pulses with reversed magnetic field have a stagnation point of the deuterium flux above the outer mid-plane and the flow velocity closed to the classical values M ~ 0.02. This result is very similar to the ones found in the EDGE2D/NIMBUS simulations without the external source of momentum. The deuterium density increases inside the last closed flux surface with the anomalous parallel SOL flow velocity. This was observed both in the simulations and experimentally. It was concluded to be an effect of the external force that changes the radial component of the deuterium flux direction at the high field side from outward to inward directed near the separatrix; creating a convective cell in the SOL and inside separatrix. While the deuterium flux was inward directed only in the region of the X-point for the plasma without the anomalous parallel SOL flow.

The change of deuterium flux direction between the outer divertor strike point and the outer mid-plane with the anomalous parallel SOL flow lead to a change of direction of the convective heat flux. This causes a drop of the total heat flux directed to the outer divertor target region and as a consequence the electron temperature also dropped at the outer divertor target plate together with the deuterium density. Electron temperature also dropped at the inner divertor target. This was due to an increase of deuterium density with the flow in the inner divertor region.

The pattern of an radial average impurity convective velocity is very similar to the radial flux of deuterium for the simulations with anomalous velocity. The deuterium particles are dragging the impurity particles from the low field side to the high field side. Particles released from the outer strike point could go very easily to the inner divertor. This is very similar to a pattern which was observed with the impurity migration where the material eroded at the outer strike point was deposited at the inner target plate [8, 11].

ACKNOWLEDGMENTS

This work, which has been supported by the European Communities and the Instituto Superior Técnico (IST) under the Contract of Association between the European Atomic Energy Community and IST, was performed under the European Fusion Development Agreement. This work was also partly funded by the United Kingdom Engineering and Physical Sciences Research Council and by the European Communities under the contract of Association between EURATOM and UKAEA. The views and opinions expressed herein do not necessarily reflect those of the European Commission and IST.

REFERENCES

[1]. Belo, P. *et al*, *Plasma Phys. Control. Fusion*, **46** (2004) 1299;

[2]. Loarte, A., *et al*, *Plasma Phys. Control. Fusion, **45** (2003), 1549*

[3]. Ongena, J. *et al*, *Nuclear Fusion*, **44** (2004) 124;

[4]. Rapp,J., *et al*, *Nuclear Fusion*, **44** (2004) 312;
[5]. Greenwald, M., *et al*, *Nuclear Fusion*, **28** (1988) 2199;
[6]. Sabini, G., *et al*, *Plasma Phys. Control. Fusion*, **44** (2002) 1769;
[7]. Erents, S.K., *et al*, *Plasma Phys. Control. Fusion*, **46** (2004) 1757;
[8]. Matthews, G.F., *et al*, *Journal of Nuclear Materials*, **337-339** (2005) 1;
[9]. Simonini, R., *et al*, *Contrib. Plasma Phys.* **34** (1994) 368;
[10]. Smick, N., *et al*, *Journal of Nuclear Materials*,†**337-339**†(2005) 281;
[11]. Fundamenski, W., et al, Nuclear Fusion, **47** (2007) 417;
[12]. Strachan, J.D., *et al*, *Journal of Nuclear Materials*, **337-339** (2005) 25;
[13]. Braginskii, S.I., in *Reviews of Plasma Physics*, ed. M.A. Leontovich (consultants Bureau, N.Y.), **1**, (1965), 445;
[14]. Strachan, J.D., *et al*, *Nuclear Fusion*, **43** (2003) 922;
[15]. Erents, S.K., *et al*, *Plasma Phys. Control. Fusion*, **46** (2000) 905;
[16]. Loarte, A, et al, *J. Nuclear Mat.*, **241-243** (1997) 118;
[17]. Loarte, A. et al, *Nuclear Fusion*, **38** (1998) 331;
[18]. Groth M., et al, *Nuclear Fusion*, **42** (2002) 1839

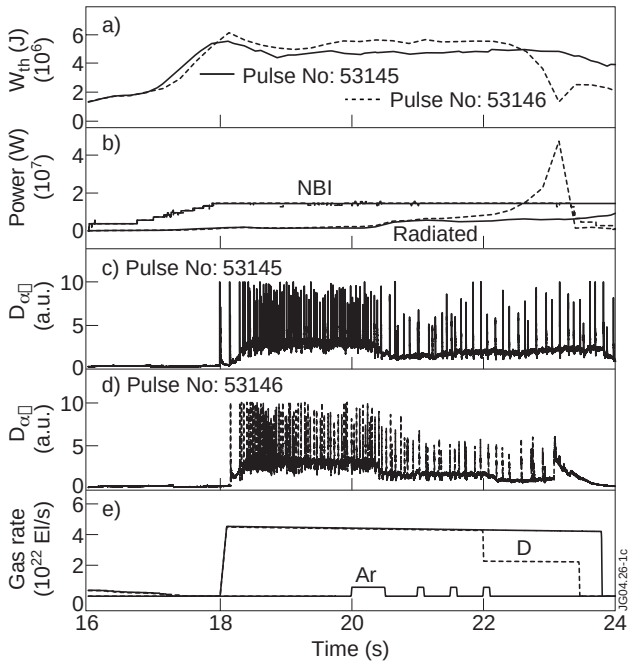

Figure 1: Time traces of selected plasma parameters for JET Pulse No's: 53145 and 53146.

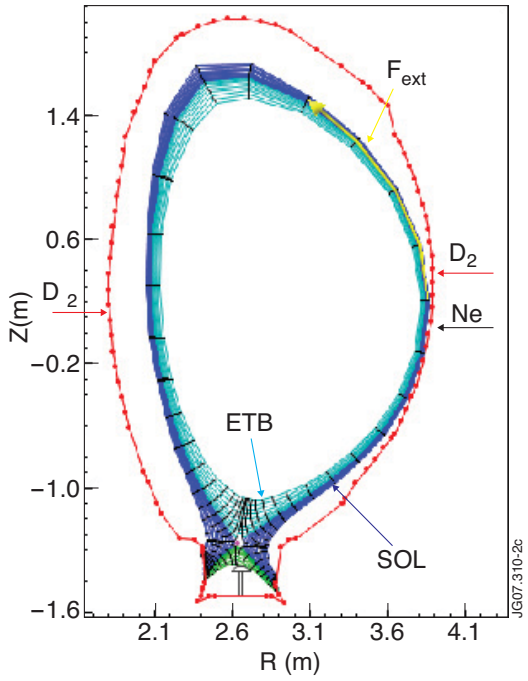

Figure 2: EDGE2D/NIMBUS computational grid, showing the location of deuterium and impurity injection. In this figure D_2 is the deuterium molecular gas, Ne is the neutral Neon, ETB is the Edge Transport Barrier, F_{ext} is the external momentum force applied to the deuterium particles in the EDGE2D/NIMBUS simulations and SOL is the Scrape-Of-Layer.

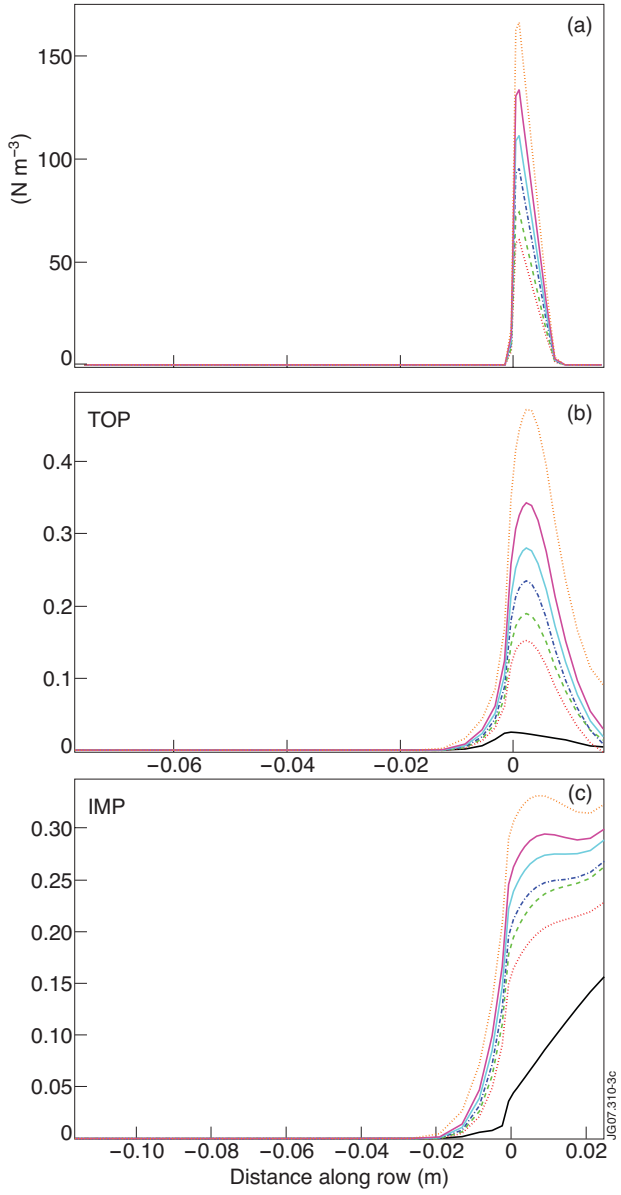

Figure 3:(a) radial profiles at the outer mid-plane of the additional parallel force on deuterium ions for different levels of external momentum injection used in the simulations. (b) The corresponding radial profile of the parallel Mach number, this time measured at the vessel top and mapped to the outer mid-plane. The Mach number at the OMP is ~ 20% smaller, but with a similar profile to that at the top of the machine. (c) The hMach number profile at the inner mid plane

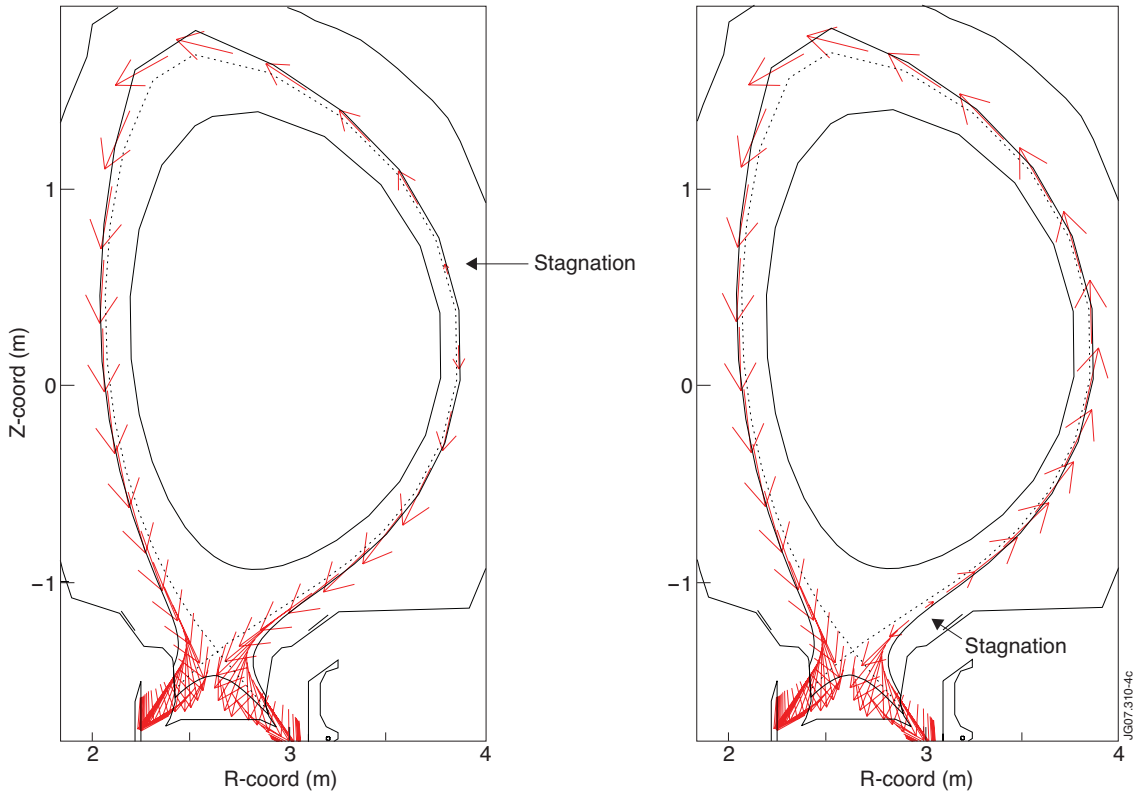

Figure 4: Arrow plot of parallel deuterium ion SOL flows, in units of $m^{-2}s^{-1}$, for EDGE2D simulations (a) without external momentum injection and (b) with maximum momentum injection. Note that the stagnation point, where $M_{||} = 0$, moves towards the outer target as a result of an increased SOL flow towards the inner target. The parallel flow is three orders of magnitude higher than the perpendicular flow, see figure 8.

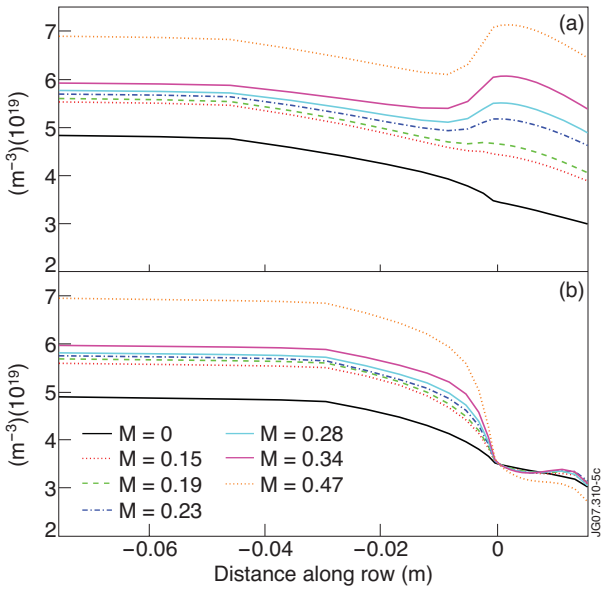

Figure 5: Radial profiles of deuterium ion density, n_i, at (a) the inner mid-plane and (b) the outer mid-plane, for different levels of external momentum injection, as measured by the parallel Mach number at the top of the vessel, see figure 3b.

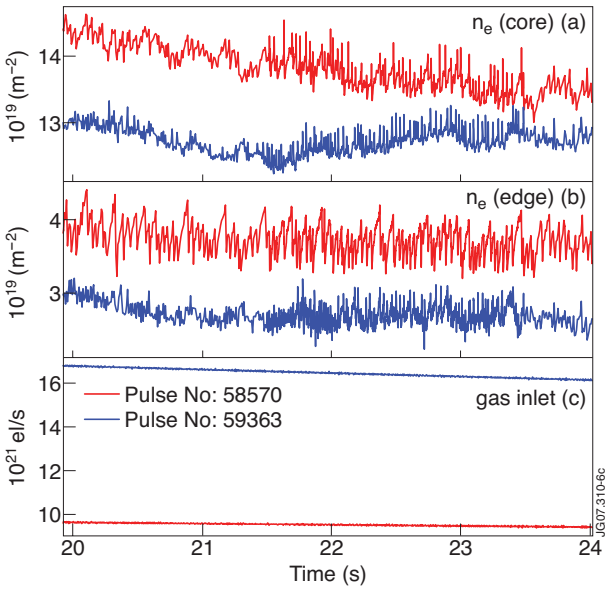

Figure 6: Time traces of (a) central ($r_{min}/a = 0.05$) line-integrated electron density, in units of m^{-2}, (b) edge ($r_{min}/a = 0.8$) line-integrated electron density, and (c) deuterium gas fuelling rate, in units of e/s. In each case the two traces correspond to similar JET pulses with (i) normal field, Pulse No: 58570, and (ii) reversed field, Pulse No: 59636.

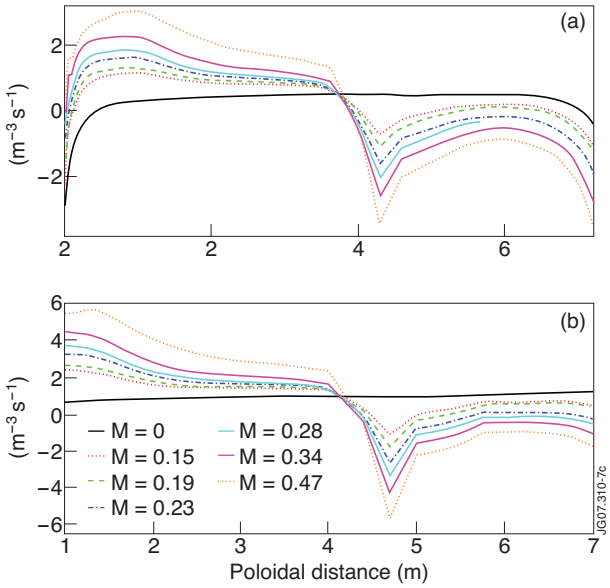

Figure 7: Poloidal profiles of perpendicular deuterium flow, in units of $m^{-2}s^{-1}$, at the first ring (a) inside and (b) outside the separatrix, for different levels of external momentum injection, as measured by the parallel Mach number at the top of the vessel, see figure 3b. The poloidal coordinate, r_p, is defined as follows: (a) inside the separatrix, $r_p = 0$ at the X-point, and (b) outside separatrix, $r_p = 0$ at the outer divertor target; in both cases, r_p increases counter clockwise in the poloidal plane, see figure 2. In the latter case, the outboard (low field side) region corresponds to $r_p = 1 – 4$ m, while the inboard (high field side) region to $r_p = 4 – 7$ m. Note that perpendicular flow is measured in the direction of r, so that outflow, e.g. from the core into the SOL, is measured as positive and inflow as negative

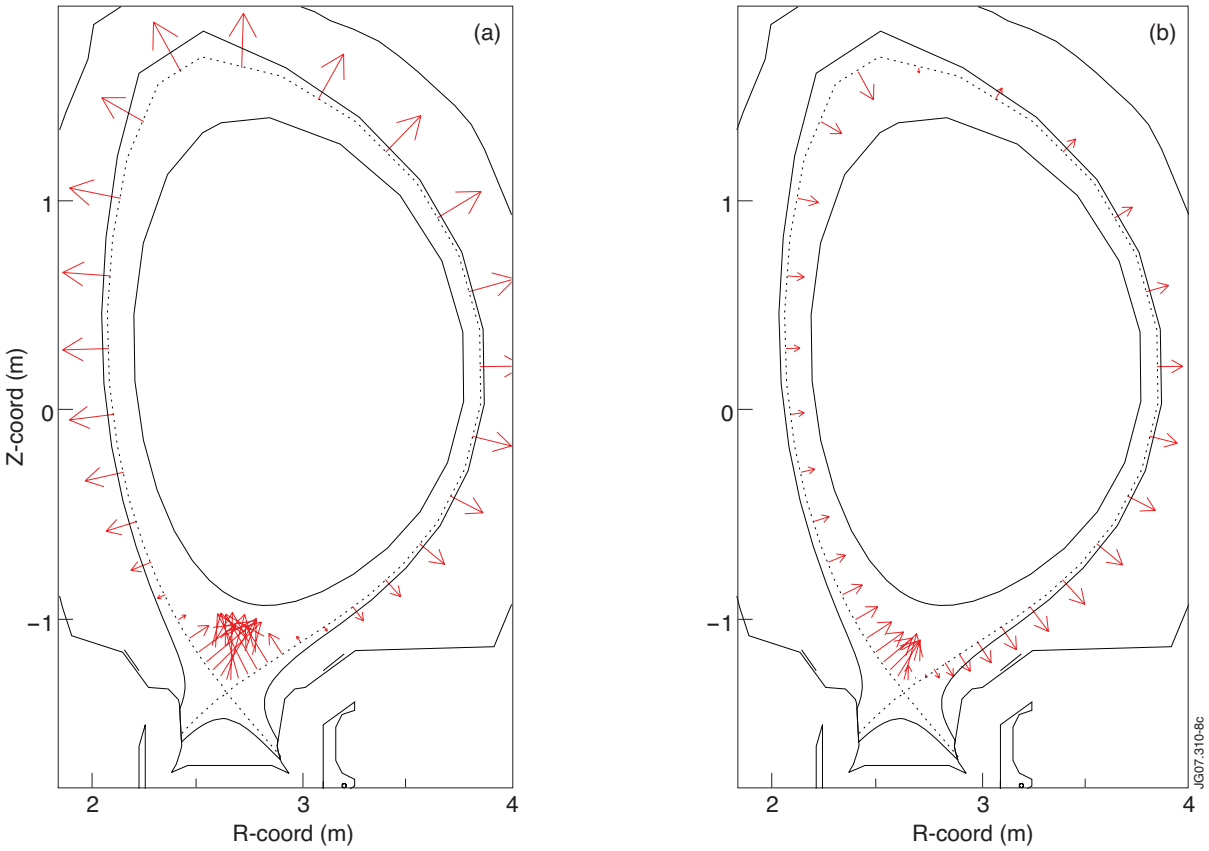

Figure 8: Arrow plot of perpendicular deuterium ion SOL flows, in units of $m^{-2}s^{-1}$, at the first ring inside the separatrix, for EDGE2D simulations (a) without external momentum injection and (b) with maximum momentum injection. Note the appearance of a re-circulating flow (global convective cell) in the latter case.

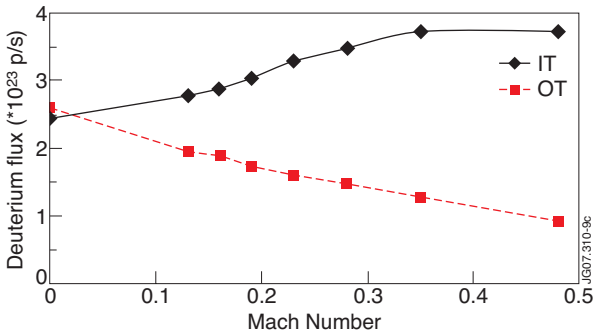

Figure 9: Integrated deuterium flow to the inner and outer divertor targets, as measured by the recycling D_α light (hence, units of photons/s), as a function of parallel Mach number at the top of the vessel, see figure 3b.

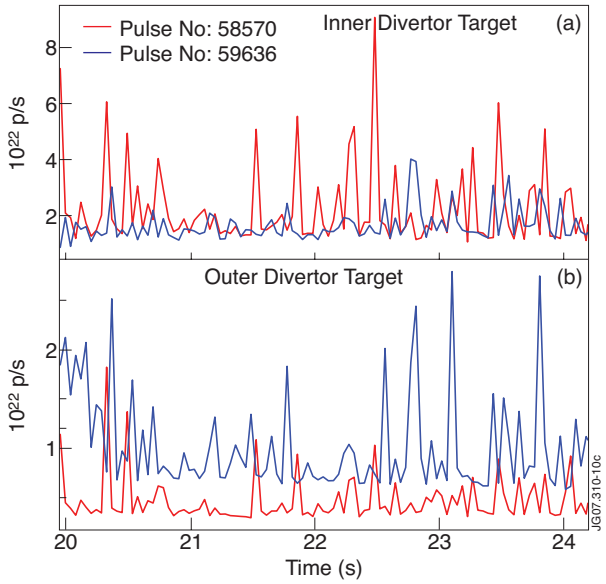

Figure 10: Time trace of the deuterium flow integrated deuterium flow to the (a) inner and (b) outer divertor targets, as measured by the recycling D_α light (hence, units of photons/s), for two similar JET pulses with (i) normal field, Pulse No's 58570, and (ii) reversed field, 59636.

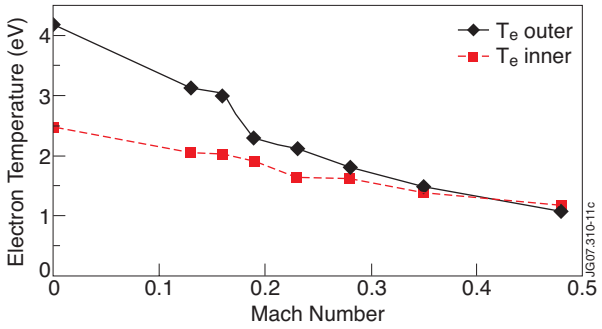

Figure 11: Electron temperature at the inner and outer divertor targets as a function of parallel Mach number at the top of the vessel, see figure 3b.

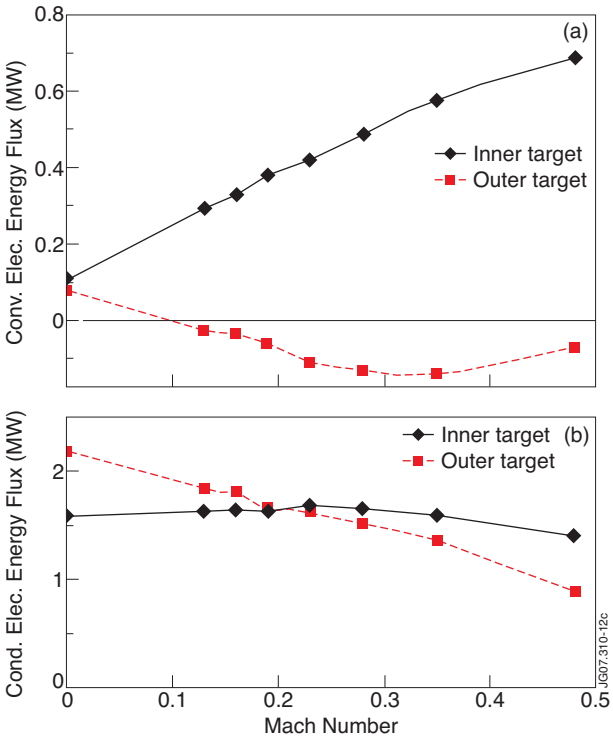

Figure 12: (a) convective and (b) conductive energy flows, in units of MW, to the outer and inner SOL divertor regions as a function of parallel Mach number at the top of the vessel, see figure 3b.

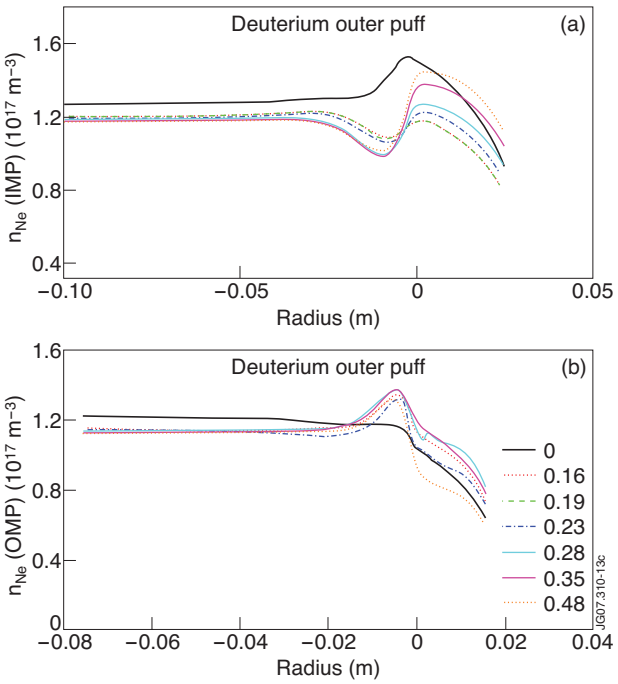

Figure 13: Radial profiles of impurity (Neon) density at (a) the inner mid-plane and (b) the outer mid-plane, for different levels of external momentum injection, as measured by the parallel Mach number at the top of the vessel, see figure 3b. The results represent simulations with deuterium fuelling from the outer mid-plane.

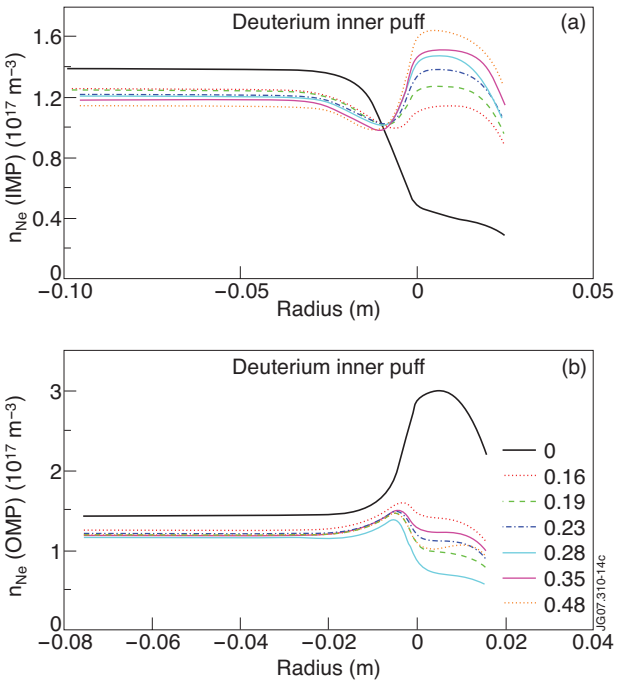

Figure 14: The same as figure 13 only with deuterium fuelling from the inner mid-plane.

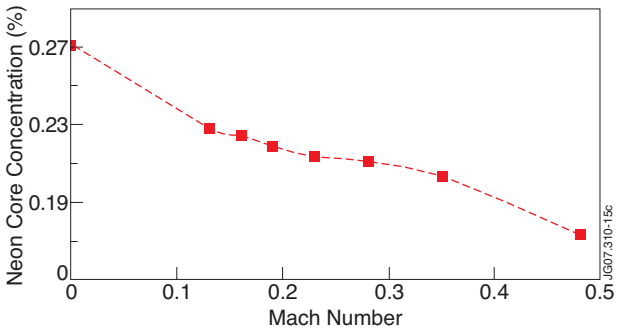

Figure 15: Total impurity (Neon) concentration inside the separatrix as a function of parallel Mach number at the top of the vessel, see figure 3b.

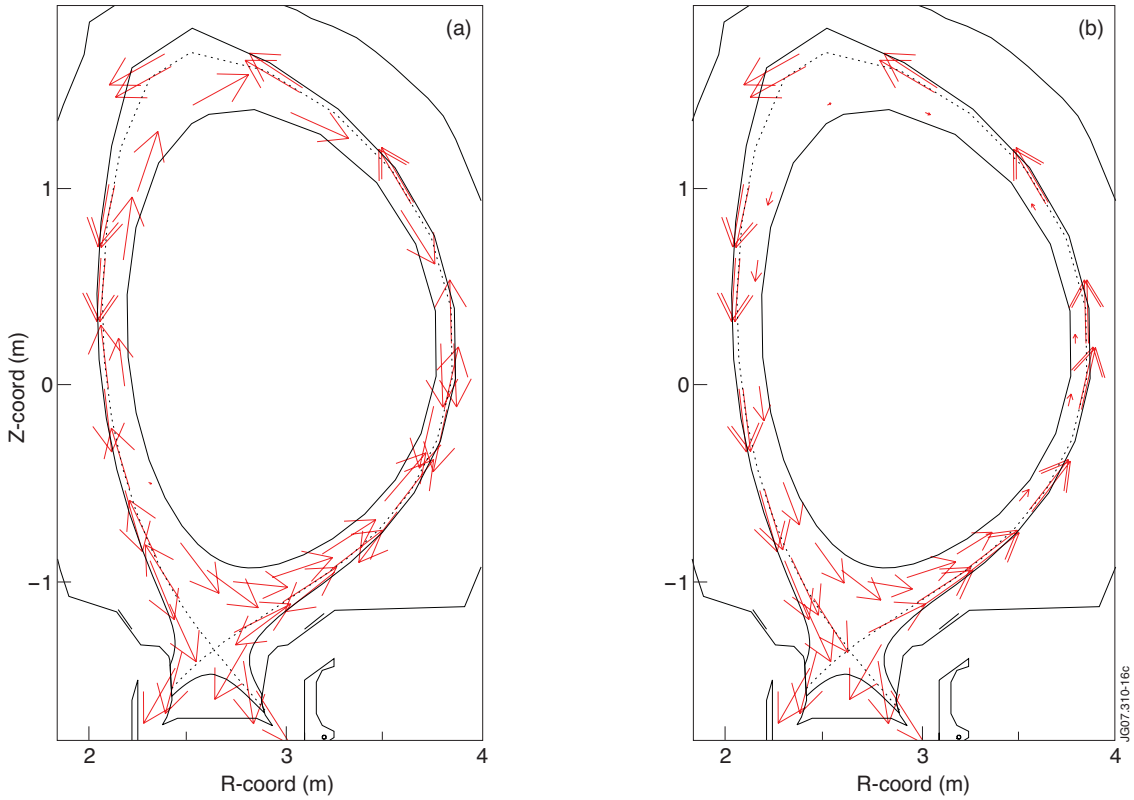

Figure 16: Arrow plot of parallel impurity (Neon) ion SOL flow velocity, in units of m/s, for EDGE2D simulations (a) without external momentum injection and (b) with maximum momentum injection. Note that the stagnation point, where $M_{||} = 0$, moves towards the outer target as a result of an increased SOL flow towards the inner target. The parallel flow is three orders of magnitude higher than the perpendicular flow

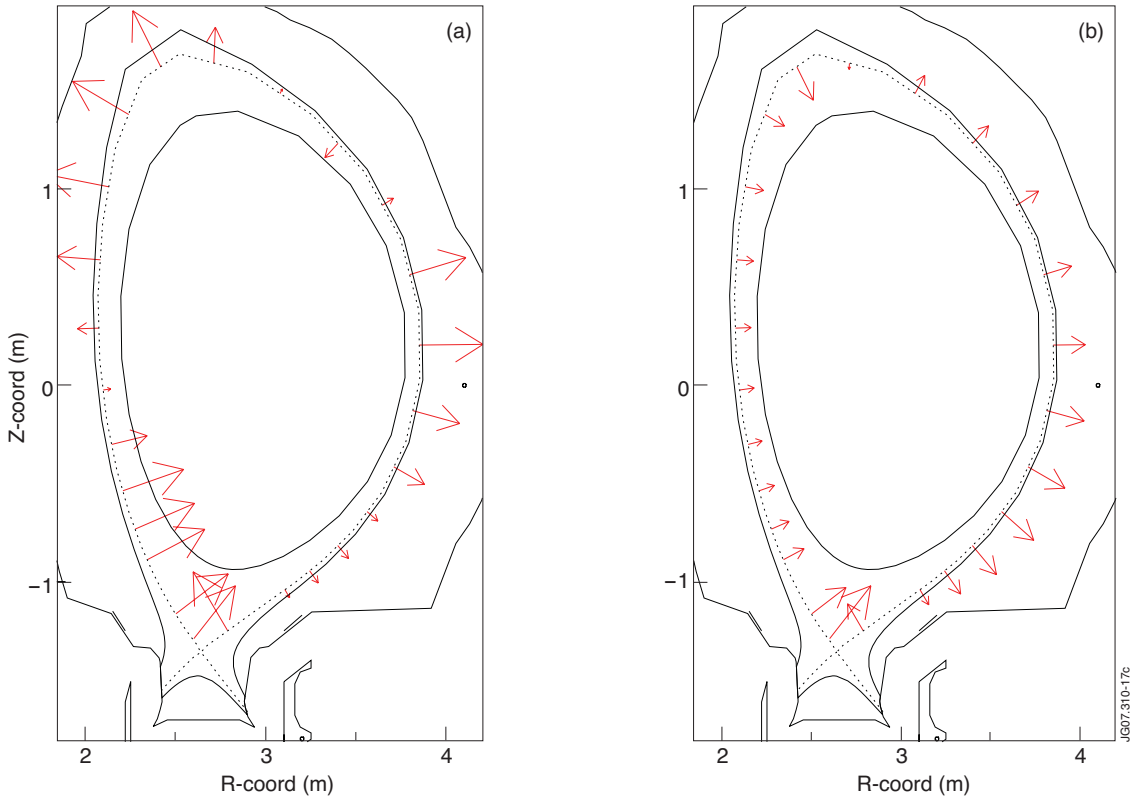

Figure 17: Arrow plot of perpendicular impurity (Neon) SOL flows, in units of $m^{-2}s^{-1}$, at the first ring inside the separatrix, for EDGE2D simulations (a) without external momentum injection and (b) with maximum momentum injection. Note the appearance of several convective cells in the first case and a global convective cell in the latter case.